Modeling 3-D Transport and Dispersal of Oil Plume Released During BP/Horizon Accident in the Gulf of Mexico in 2010

Konstantin A. Korotenko[1,*], Malcolm J. Bowman[2], David E. Dietrich[3], and M. Hamish Bowman[4]

[1]*P.P. Shirshov Institute of Oceanology, Moscow, Russia*
[2]*School of Marine and Atmospheric Sciences, State University of New York, Stony Brook, NY, USA*
[3]*San Diego State University Computational Science Research Center, San Diego, CA, USA*
[4]*Department of Marine Science, University of Otago, Dunedin, New Zealand*

Received September 14, 2012; Accepted November 10, 2012

Abstract: A circulation/oil spill model based on the DieCAST Ocean Circulation Model and the Oil Spill Model has been applied to the Gulf of Mexico to address the transport, fate and 3-D structure of the oil plume resulting from the accidental Deepwater Horizon spill in April-September 2010. Surface forcing is based on annual cycle climatology. However, on the start date of the blowout, climatological winds are replaced by regional 32 km 3-hourly NARR re-processed winds over the entire Gulf. The results from the modeling approach suggest that the prevailing synoptic winds played a major role in pushing the oil toward the Gulf northeastern coasts, and, in synergy with the Loop Current variability, prevented the oil from passing through the Florida Straits to the Atlantic Ocean. Simulations showing the shape and extent of the surface slick are compared with available visible satellite imagery and give interesting results.

Keywords: circulation/oil spill model, deepwater oil well blowout, effect of winds, Gulf of Mexico

1 Introduction

The British Petroleum (BP) Deepwater Horizon oil spill (also known as the Gulf of Mexico (GoM) Oil Spill or the BP Oil Spill) in April-September 2010 was the largest marine oil spill in history, and has proved to be a multifaceted disaster, with simultaneous developments on the surface of the water and at the wellhead about 1,500 m below, at the site of the Deepwater Horizon (DWH) explosion and on shorelines

*Corresponding author: kkoroten@yahoo.com

DOI: 10.7569/JSEE.2012.629504

from Texas to Florida, affecting wildlife, oil workers, tourism workers, and everyone who cares about the wealth of natural resources along the Gulf Coast [1–3].

1.1 History of the BP Accidental Oil Spill

The DWH offshore oil platform was located in the Mississippi Canyon Block 252 (MC252) of the GoM, approximately 50 nautical miles (93 km) southeast of the Mississippi River delta (28.74°N, 88.39°W). After explosion on April 20, 2010, the platform sank in about 1,500 m of water. The sinking of the platform caused crude oil to gush out of the riser, the 1,500 m pipe that connects the well at the ocean floor to the drilling platform on the surface. After a series of failed efforts to plug the leak, BP said on July 15 that the oil well was sealed that stopped the flow of oil into the Gulf of Mexico for the first time in 86 days. According to [4], the emerging consensus is that roughly five million barrels (~0.7 million tons) of oil were released by the Macondo well, with roughly 4.2 million barrels (~0.57 million tons) pouring into the waters of the GoM.

It was estimated that 8,400 m^3 of oil and gas per day were escaping from the well just before it was capped [5]. It is believed that the daily flow rate diminished over time, starting at about 9,900 m^3 per day and decreasing as the reservoir of hydrocarbons feeding the gusher was gradually depleted. On September 19, the relief well process was successfully completed and the federal government declared the well "effectively dead." According to [6], the average flow rate after riser removal was about 1.7×10^{-2} and 1.1×10^{-1} m^3 s^{-1} for the lighter and darker flows, respectively, or 1.2×10^{-1} m^3 s^{-1} total, while before riser removal it yielded a flow rate of 1.0×10^{-1} m^3 s^{-1}.

The DWH blowout at the MC252 Macondo well site lasted nearly three months. To reduce the impact of the surface oil reaching sensitive coastal environments, chemical dispersant was applied through surface application and subsurface direct injection into the wellhead. The objective of dispersant use is to minimize the amount of surface oil that reaches shoreline habitats, where it threatens a wide range of animals and plants. As was estimated in [5], 8% of Macondo oil discharged in GoM was chemically dispersed in addition to 16 % of the oil dispersed naturally.

The oil slick produced by the DWH oil spill covered as much 75,000 square kilometers, an area about the size of South Carolina, with the extent and location of the slick changing from day to day depending on weather conditions [1]. By the first week in June, oil had come ashore in Louisiana, Mississippi, Alabama, and Florida, with significant wildlife fatalities in Louisiana. In the weeks following the accident, scientists discovered enormous oil plumes in the deep waters of the GoM [7–9], raising concerns about ecological harm far below the surface that would be difficult to assess.

Figure 1 shows a cumulative oil slick footprint at the sea surface indicating that, during the blowout, the oil slick spanned the most of northeastern Gulf while an insignificant part of the oil slick, driven by the Loop Current, approached to the

DOI: 10.7569/JSEE.2012.629504

Figure 1 The cumulative slick footprint for the BP/Deepwater Horizon oil spill with the location of the BP rig. The footprint has been created by overlaying all of the oil slicks mapped by SkyTruth on satellite images taken between April 25 and July 16, 2010 (after [3]).

Florida Strait. Satellite observations of the surface oil slicks and sheen from April 25 through July 16 showed that, at one time or another, ~240,000 km^2 of Gulf waters were covered with oil [3]. However, the cumulative oil slick footprint did not include the distribution of hydrocarbons suspended in the water column, dissolved in the water, or driven beneath the surface by the application of chemical dispersants. Note that ocean currents at depth potentially transported that material in different directions than oil at the surface, making it likely that the total area of the Gulf spill was larger than the cumulative oil slick footprint determined from satellite image analysis.

It should be emphasized that the majority of known and documented large oil spills were spilled either at the sea surface or from shallow water blowouts [9, 10]. The initial dimensions of the latter were mostly determined by the flow of gas released with the oil. The gas, rising to the surface as a column of bubbles, acts as a large-scale pump to quickly transport of oil droplets to the surface. Because the normal ocean currents are small compared to the vertical rise velocities in the plume, they have little influence on oil droplet displacements. This may be different when considering a subsea oil well blowout in deep water, as in the case of BP Oil Spill. In this situation, the high pressure and low temperatures may cause the natural gas to combine with water to form a solid, ice-like substance known as hydrates [11]. The gas volume may also be depleted through dissolution into the water. With the loss of gas through either or both of these processes, the driving buoyancy of the rising plume may be completely lost, which will result in the oil droplets rising slowly under gravity forces alone. The movement of the oil droplets will now be affected by cross currents during their rise [11, 12]. This will result in the separation of the oil droplets based on their drop size. The large diameter oil drops will surface first, and smaller drops will be carried further down current

DOI: 10.7569/JSEE.2012.629504

prior to reaching the surface. Oceanic diffusion processes will result in additional separation of the oil drops due to their varying residence times in the water column [11, 12]. The application of dispersant considerably changes the 'natural' oil droplet size distribution reducing size and buoyancy of oil droplets. Thus, more droplets are likely to be trapped in subsea layers and/or deposited.

In the general case, deep well blowout or leakage will release two buoyant fluids into the seawater: oil and natural gas. The gas phase is highly buoyant; the oil phase is moderately buoyant. The combined buoyancy will drive a three-phase plume (oil, gas, and sea water), which will rise toward the surface [13]. En route, plume transport will be affected by interactions with the ambient ocean including: (1) entrainment of seawater into the plume; (2) physical-chemical reactions between seawater and both gas and oil; (3) sub-surface intrusion of portions of the plume; and (4) surface spreading of remaining portions of the plume. These phenomena and other complex mechanisms, such as jet instability and break-up, that influence plume generation and its transport to the sea surface are not completely understood and need specific approaches to deep oil spill modeling [14].

1.2 Modeling Approaches for Prediction Behavior and Fate of Macondo Oil

Despite the tragic event, the BP accident put a challenge to oil spill modelers to predict realistically oil fate and movement in the GoM. In addition to specific algorithms sensibly describing fate of oil, ocean circulation models coupled with oil spill models should realistically predict ocean currents. A keystone for this is to use reliable background and atmospheric forcing. No matter how good the model would be, ignoring the local wind forcing leads to errors in predicting of oil plume behavior and the concentration distribution. This was illustrated by a number of numerical studies performed at the beginning of the BP incident when a large amount of oil was predicted to pass through the Florida Strait and, further, driven by the Gulf Stream, contaminated significant part of the southeastern Atlantic coast of the U.S. (see results obtained in [10] with CCSM model). Incorrect results associated with neglecting local winds were also obtained in [15] with the coupled SABGoM/LTRANS model. The results of simulation of the Macondo oil spill in upper 200 m layer did not reveal oil beached at the northeastern coast of the Gulf that contradicting with observations. One can find more results of numerical simulations contradicting to observation in [16, 17]. Another cause of discrepancy between model results and observations of the Macondo oil slick could be incorrectly predicting mesoscale water circulation and eddies. As was found in [18], among simulated daily oil slicks presented on the site http://gohsep.la.gov/oilspill.aspx, almost all simulated slicks were far from reality because the water vortex dynamics were ignored in the simulations.

DOI: 10.7569/JSEE.2012.629504

Authors of this work seemed to be the first modelers who paid much attention to synoptic winds that could play a crucial role in spreading the BP oil spill at the surface [19]. For predicting the Macondo oil slick transport and dispersal at the sea surface, we forced our coupled ocean circulation/oil spill model, for the period of accident, with regional synoptic 3-hourly NARR[1] winds. The results indicated the major role of the local winds in movement of the oil slick toward the northeastern GoM coast and the minor role of the Loop Current in the transport of oil toward the Atlantic Ocean. Recently, researchers from RSMAS (UM), using GoM-HYCOM model coupled with an oil spill model, revealed the similar effect with local NODC winds [20].

In this work, we focus on 3-D structure and evolution of the BP oil spill, taking into account formation of the oil plume during its rising from Macondo well and spreading at the sea surface. In deepwater, the movement and fate of the plume is governed by terminal velocity, background currents and stratification, while, at the sea surface layer, the plume evolution and fate undergo influence of currents induced by local synoptic winds, Stokes drift and physico-chemical mechanisms affecting the oil properties. We do not study effects of dispersants applied at the surface and directed to the Macondo wellhead during the incident, since their role in quantitative characterization of the Macondo subsea plume was not well understood yet.

The paper is organized as follows: In section 2, we briefly describe features of mesoscale circulation in the GoM and NARR winds. In section 3, we present the ocean circulation/oil spill model and processes affecting the transport and fate of oil. In section 4, we present and discuss results of simulation of GoM circulation and evolution of the BP oil spill. Conclusion is given in section 5.

2 Features of Mesoscale Circulation of the GoM

The main feature of the GoM is the strong Loop Current, which flows into and out of the Gulf and is classified as a western boundary current. In 1947, Henry Stommel of the Woods Hole Oceanographic Institution first recognized the essential role the latitudinal variation of the Coriolis force plays, along with the location of the major wind belts (trades and the higher-latitude Westerlies) in establishing and driving these intense ribbons of rapidly flowing waters. Western boundary currents are found along the western boundaries of the major ocean basins (e.g., the Kuroshio Current in the northwestern Pacific, the East Australian Current in the southwestern Pacific, the Brazil Current in the southwestern Atlantic Ocean and the Gulf Stream in the northwest Atlantic). The Loop Current is derived from the Caribbean current, which flows through the Caribbean Sea, becoming the Yucatan Current as it enters the GoM between the Yucatan Peninsula and Cuba. The Loop current

[1] NCEP North American Regional Reanalysis (http://www.emc.ncep.noaa.gov/mmb/rreanl/)

DOI: 10.7569/JSEE.2012.629504

has many interesting and important characteristics. Bulging into the GoM like a giant aneurysm, huge clockwise-rotating anticyclonic eddies continually break off into Loop current eddies every 6 to 12 months. These eddies contain vast amounts of heat and kinetic energy and typically penetrate down to 600 m. Since they are comprised of lower density tropical water, the eddies are buoyant and are easily detected from satellites by their temperature, color and surface elevation (http://www.aoml.noaa.gov/phod/dhos/altimetry.php).

As show in Figure 1, the DWH platform was located between the edge of the northern GoM shelf and the Gulf interior. This is an area where the ambient circulation is affected by the regional open sea dynamics, dominated by the Loop Current and associated eddy field, and by shelf processes, largely affected by Mississippi-induced buoyancy driven and wind-driven flows. The Loop Current eddies, once disentangled from the Loop Current itself, then slowly drift westward for several months before colliding with the western continental shelf of the Gulf. So a detailed understanding of the nature and dynamics of the Loop Current and its eddies is fundamental to understanding how deep contaminants will be transported away from the spill wellhead site and eventually mixed into the world ocean.

3 Description of the Coupled Model

3.1 The DieCAST Circulation Model Adjusted for the GoM

The regional 1/8 deg low dissipation GoM DieCAST (DieGoM) ocean circulation model was developed as module to prescribe current velocity, V, temperature, T, and salinity, S, necessary for GoM Oil Spill Model (GOMOSM) offline run. DieGoM model grid area (142 × 186 grid) covers a region from 99.94° to 82.56°W and from 8.78° to 39.19°N that includes the GoM.

DieGoM was initialized by Levitus climatology and run under Hellerman–Rosenstein winds and daily V, T, S data provided by the 1/4 deg resolution global DieCAST model (http://efdl.as.ntu.edu.tw/research/diecast/index.html) at open boundaries in the central Caribbean Sea and Eastern Florida Strait. Both circulation models have 26 unevenly spaced z-levels with smaller intervals chosen near the surface for better representation of surface processes. The levels with interfacial depths are situated at: 0, 13.3, 28.2, 45.1, 64.3, 86.6, 112.3, 142.5, 178.1, 220.1, 270.2, 330, 401.8, 488.1, 592.1, 717.9, 870.2, 1054.9, 1279.2, 1551.8, 1883.4, 2287.1, 2778.9, 3378.2, 4108.9, and 5000 m. Along the bottom, which consists in a series of horizontal steps, the vertical velocity is set to zero.

Both models calculate control-volume averages of horizontal momentum, potential temperature and salinity. The vertical velocity is derived from the incompressibility equation after preliminary calculation of the horizontal velocity in a way that forces the divergence of the barotropic mode to match that implied by the specified

DOI: 10.7569/JSEE.2012.629504

vertical velocity at the surface. This surface vertical velocity is prescribed as a combination of net evaporation minus precipitation. On the start date of the blowout, climatological winds, in the DieGoM, are replaced by regional 32 km 3-hourly NARR re-processed winds over the entire Gulf, in order to provide more realistic surface stresses on the floating constituents of the oil slick.

3.2 The GoM Oil Spill Model

The GOMOSM uses the 142 × 108 grid covering the GoM from 99.94° to 82.56° W and from 18.2° to 30.4°N. For the sake of reducing computation cost, 78 southernmost grid lines of DieGoM were removed in order to cover only the Gulf. The non-uniform vertical resolution of the GOMOSM with 600 layers is chosen to set the highest resolution (0.1 m) in the uppermost layer. During dataset transfer from the DieGoM to the GOMOSM, the former was preliminarily interpolated onto the vertical grid of the latter. The processes affecting the oil transport and fate to be modeled in the GOMOSM are described below.

3.2.1 Processes Affecting an Oil Plume

As was mentioned above, the catastrophic event in the GoM left the Macondo well flowing without control into its surrounding waters. Large volumes of crude oil and natural gas began to be released into the environment from wellhead at 1522 m depth. Elevated gas fluxes, associated with the oil flow, affect the oil transport and fate through the water column. Submerged oil and gas are transported by deep currents and may impact a large region of the GoM, including the shelf water. In [21], study of deep oil blowouts indicated that blowouts at depths greater than 900 meters resulted in a very fast conversion of all of the gas to ice-like substance known as hydrates. The gas volume may also be depleted through dissolution into the water. With the loss of gas through either or both of these processes, the driving buoyancy of the rising plume may be completely lost, which will result in the oil droplets rising slowly under gravity forces alone. The movement of the oil droplets will then be affected by cross currents during their rise. This will cause the oil plume to bent and result in the separation of the oil droplets based on their size. The large diameter oil droplets will surface first and smaller droplets will be carried further down current prior to reaching the surface.

In deepwater, the mechanism of the oil-gas separation is very important, since it directly affects an oil plume rise velocity. Because gas rises faster than oil, it separates the former from the bent plume. Time of separation of gas from oil (transient time) is very important characteristic for multiphase plumes, and there are many models that were proposed [22–26] for its estimation. After gas is separated from the plume, usually taking several seconds [26], a Lagrangian parcel method is used to track the transport of gas, hydrate, and oil in what is called far field conditions.

To track an oil plume from deep releases, one needs to know the oil droplet size distribution, the droplet rise velocities, the ambient water current and density, and

DOI: 10.7569/JSEE.2012.629504

oceanic diffusion processes. In [27], the droplet rise (terminal) velocities have been determined as

$$u_t = \left(4gD_p(\rho_p - \rho)/(3\rho C_D)\right)^{1/2} \quad (1)$$

where u_t is terminal velocity of an oil droplet, g is the gravitational constant, D_p is the diameter of a droplet, ρ_p is density of oil, and ρ is density of water. C_D is drag coefficient, which is equal to $24/N_{\mathrm{Re}}$ for $N_{\mathrm{Re}} < 0.1$ or equal to $(24/N_{\mathrm{Re}})(1+0.14N_{\mathrm{Re}}^{0.7})$ for $N_{\mathrm{Re}} < 1000$, where $N_{\mathrm{Re}} = D_p\rho_p u_t/\mu$ ($\mu$is the dynamic viscosity fluid). From Eq. (1), we can estimate average terminal velocity for Macondo crude oil (MC-252).

Notably, according to (1), droplet size does not determine the equilibrium level. The terminal velocity vanishes at the equilibrium level, where the bulk material density matches the ambient water (also according to Archimedes' Law). However, droplet size affects its terminal velocity and thus the time it takes to reach its equilibrium level. In the long run, the equilibrium level is as important as the time it takes the droplet reach it. The smaller the droplet, the longer it takes, thus giving the underlying currents longer time to affect its path on the way to the equilibrium level, and thus separating the paths of droplets having the same bulk material density but different diameters, even when they start at the same wellhead location and time, as the underlying currents also evolve.

Taking into account that MC-252 oil is light paraffinic crude oil with average density and viscosity 0.83 kg l^{-1} and 4cP, respectively, one can estimate rise time from Eq. (1). So, for example, largest oil droplets (300 μm) will be rising from 1500 m during 6 hr [21]. Since oil droplets have a range of sizes, they have different terminal velocities, and, thus, reach the surface at different times after discharge. They also reach the surface at different spots because the droplets are subjected to cross-currents that cause smaller droplets to be swept further down-current than large droplets. This droplet separation is further complicated by the fact that eddies and currents in the water can vary both spatially and temporally. At the surface, oil droplets are moved away from initial points by currents, winds, and waves that result in forming oil slicks.

Once oil reaches the sea surface, a number of specific factors affect its properties, transport, and dispersal, in addition to those affecting its path as it rose through the underlying flow. Among them, processes of evaporation, emulsification, and photolysis are controlled by properties of the oil itself. Different processes sequentially dominate as the plume evolves over time following the spill, eventually lead to a complete loss of the oil mass. In [28], the relative importance of the various processes active, over time, on the mass of an oil spill is illustrated. For example, evaporation, dispersion, and emulsification are important during the early stages, while biodegradation, photolysis, sinking, and tarball formation become important later over a period of days and months and even years. Depending on the grade of the oil, the relative effects of photolysis and biodegradation to the mass balance may be small in comparison with the evaporation, dispersion, and emulsification processes. Approaches for modeling

DOI: 10.7569/JSEE.2012.629504

abovementioned processes in Lagrangian oil spill models were demonstrated in authors' work [29–31] and in a large number of publications by other researchers (see overview in [29]).

In the GOMOSM, special attention is paid to the process of advection that acts over all phases of oil slick evolution. The advective transport of the oil slick is governed by the seasonal circulation, buoyancy-driven and wind/wave induced currents. In general case, the advection due to the combination of these components is defined as vector sum

$$V_i = V_i^{wid} + V_i^{wad} + V_i^d + V_i^c + V_i^B \tag{2}$$

where V_i^{wid} and V_i^{wad} correspond to velocity due to wind drift and wave (Stokes) drift component, respectively which, generally, do not coincide in direction; V_i^d is the time average velocity of the wind-induced component, V_i^c denotes the climatological average component, and V_i^B is the buoyancy driven component. For the sum of the wind-induced and Stokes drift components, $V_i^{wid} + V_i^{wad}$, we chose a simplest parameterization [32] and expressed it in terms of the wind speed U_A (NARR winds) at 10 m above the water surface: $V_i^{wid} + V_i^{wad} = 0.03U_A$.

The basic concept of the present oil spill model is similar to that presented in [31], where oil is initially divided into fractional hydrocarbon groups to describe the evaporation process with more accuracy [33].

The Macondo oil (MC-252) is light paraffinic crude (0.83 kg l^{-1}) oil with low wax content (1.6 weight %), low ashaltene content (0.2 weight %), low viscosity (4cP at 32°C) and low pour point (–27°C). As was estimated by Daling [34], the total evaporative loss of MC 252 at the sea surface is about 55% within 5 days. Emulsification properties of oil are the following: (1) slow water uptake rate occurs during the first (1–3) days, (2) stable emulsion is formed after 3–5 days (maximum water is about 75%), and (3) slow viscosity development (< 10.000cP after 1 week at sea). These parameters were used in the GOMOSM.

The procedure of predicting oil spill behavior is divided into two parts: i) predetermination of currents, temperature and salinity with the DieGoM hydrodynamic model; and ii) applying these three-dimensional fields to the behavior of individual oil droplets, the aggregate of which constitutes the oil plume. The model, thus, simulates the advection, turbulent diffusion and physicochemical decay processes that change the oil plume structure and properties using pre-described temperature and salinity. Suggested in [35], the emulsification is modeled on the approach, which simulates the process of formation of "water-in-oil" mousse. The oil spill is represented by individual particles (droplets) mimicking oil displacement and fate based on oil characteristics and droplets parameters.

3.2.1.1 Synoptic Winds

Local winds played a great role in oil slick movement during the blowout period and, as it was stated above, prevented the oil passing through the Florida Strait to

DOI: 10.7569/JSEE.2012.629504

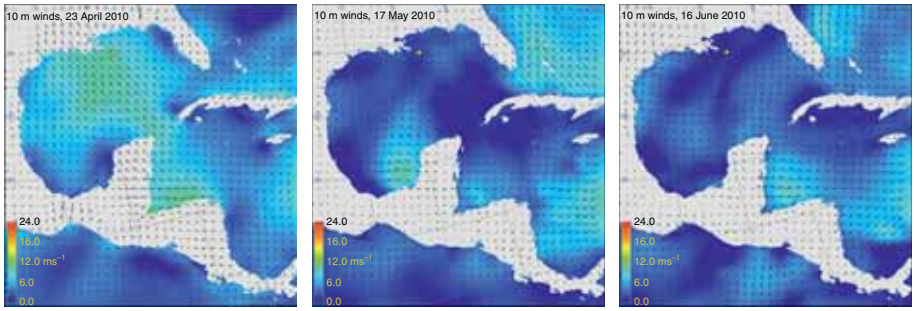

Figure 2 Samples of daily averaged NARR winds over the Gulf on 23 April, 17 May and 6 June 2010.

the Atlantic Ocean. Figure 2 shows samples of daily averaged NARR winds over the Gulf on 23 April, 17 May and 6 June 2010 indicating that from April to June, dominant winds, in the area of BP/Horizon rig, were blowing from the southeast. However, in that period the southeasterly winds were interrupted periodically by winds from other directions as well as by calm periods, one of which, shown on 17 May, is characterized by weakening winds. This calm period spanned from 16 to 20 May and, as will be shown below, led to intriguing movement of oil slick when a long ribbon of surface oil stretched far to the southeast.

3.2.1.2 GOMOSM Setup

Before simulating the transport of an oil plume, a number of initial parameters should be specified. Besides the abovementioned parameters provided by Daling [34], we also specified droplet diameters $d_{\min}$ = 2.5 μm and $d_{\max}$ = 400 μm, as well as 'half-life times' $T_{ev1} = 20\,\text{hr}$, $T_{ev3} = 30\,\text{hr}$, $T_{ev5} = 10\,\text{hr}$, for the hydrocarbon groups C^5, C^1 and C^3, respectively. For the 'long-living' groups, C^2, C^4, C^6 C^7, and C^8, we set $T_{ev4} = 250\,\text{hr}$. A percentage ratio between *C*-groups, which a priori was set initially during a distribution of droplets between groups for the light crude MC-252 oil was the following: C^1 = 15%; C^2 = 20%; C^3 = 25%; C^4 = 10%; C^5 = 15%; C^6 = 3%; C^7 = 7%; and C^8 = 5%. These percentages mean that about 55 weight % of oil will be evaporated within the first few days after it reaches the sea surface (cf. [34]). According to the percentages and weight of the hydrocarbon groups, oil density was assigned randomly around the mean density of each group. Droplet diameters are set as a bimodal distribution between $d_{\min}$ and $d_{\max}$ with the two local maxima at 10 and 300μm. In this study, we did not work on effects of the application of dispersants, which alters size and bulk material density distribution of the bonded oil and dispersant material.

3.2.1.3 Oil Source

For modeling, we set the oil source at 28° 44′ N, 88° 23′ W at 1522 m. Since the estimated separation height between oil and gas was 300 m above the Macondo

DOI: 10.7569/JSEE.2012.629504

wellhead [12] and terminal velocity of oil droplets driven by gas bubbles was very high [26], we distributed oil droplets in a vertical 300 m column above the wellhead (distributed source). It appears to be a more correct definition of the oil source than to use a point source situated above the separation height, as is set in [20].

Simulations of oil plume span 2 months from the beginning of oil discharge on 20 April 2010. For that period, oil spill rate ranged from about 200 tons/day, at the beginning of the accident, to 6000 tons/day, at the end of simulations. In the model, we set the uneven spill rate according to the Congressional Research Service Report [36] and released a corresponding number of particles every half an hour (the time step of the Lagrangian integration) to follow oil mass discharged. The total number of the particles, launched in the model, usually does not exceed 10^7; nevertheless, the behavior of the tracked particles proved to be representative of the entire spill, even though each droplet represents only an infinitesimal part of the total oil volume. According to oil budget estimates given in [36], we corrected the amount of oil in the ascending plume taking into account approximated oil mass left trapped in deep layers due to the application of dispersants at the point where oil was escaping the wellhead, affecting the fate of oil material elements that have bonded to the dispersants, because of their altered size and bulk material density change their buoyancy equilibrium depth as well as the time required for them to migrate that depth.

At the moment of each release of particles, the distribution of their "half-life" in hydrocarbon groups is assigned randomly by a random number generator. The generator gives uniform choices distributed uniformly between 0 and 1. The initial uniform distribution is transformed into an exponential distribution with a weight dependent on current wind speed magnitude at the sea surface and oil temperature [37]. Such an approach was found to be good for realistic modeling of evaporation processes. Note that only particles that occur within the subsurface 'evaporation layer' of thickness 0.1 m, i.e., in the uppermost model layer, experience evaporative decay, while particles at all depths in the water column experience only disintegration by other processes [30].

3.2.1.4 Boundary Conditions

The model takes into account the beaching and depositing of oil droplets: if an oil droplet reached the coastline or bottom, it was marked as beached or deposited, respectively. In that case, the droplet was 'frozen' at the point where it reached the boundary; otherwise, the droplet was reflected back to sea and remains in the computational process.

More structure details on the model are given in [30]. Here, in Figure 3, we just show the schematic of the GOMOSM coupled with DieGoM. Schematic blocks illustrate the sequence of the computation process of modeling transport and fate of oil spill.

Results of modeling are presented in the oil concentration, kg m^{-3}, estimated as the number of oil droplets found in the model grid cell relative to the volume of

DOI: 10.7569/JSEE.2012.629504

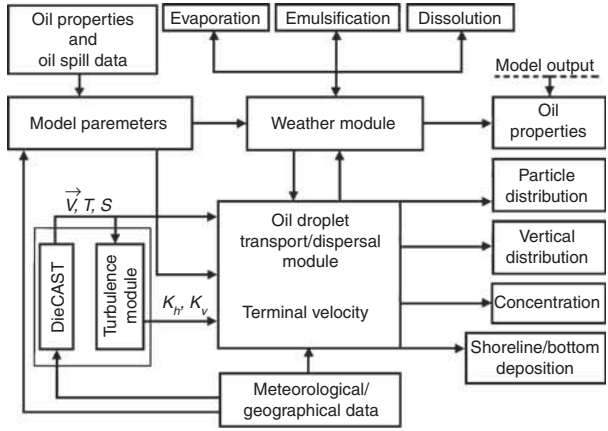

Figure 3 Schematic of principal elements of the coupled model GOMOSM/DieGoM.

the cell. In the "Model Output" block, the particles remaining in the water column, at the sea surface, beached, and decayed are counted separately and inventoried in an updated summary. For 3-D representation of the ascending plume, we stored coordinates of each oil droplet in the plume at each time step.

4 Results and Discussion

Below we present numerical reproducing water circulation and distribution of oil discharged from Macondo well in 2010. As was mentioned above, the period of simulations started on 20 April 2012 and ended approximately a month before the wellhead was sealed.

4.1 Modeling the GoM Circulation

Figure 4 presents the sequence of the computed sea surface height (SSH) snapshots on year days 125, 137, 155, and 170 corresponding to 5 May, 20 May, 5 June, and 20 June 2010, respectively. As seen, at the beginning of the BP Oil Spill accident,

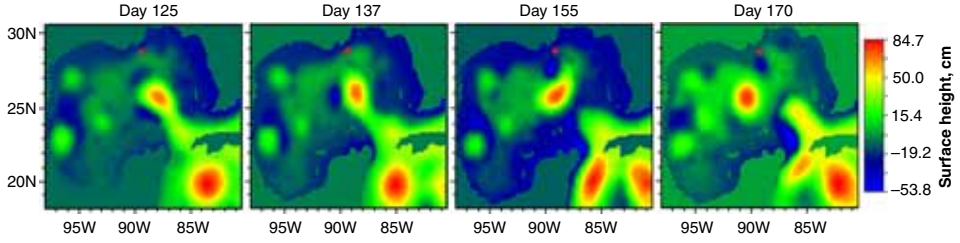

Figure 4 Sequence of the SSH snapshots computed for year days 125, 137, 155 and 170.

DOI: 10.7569/JSEE.2012.629504

in early May, the Loop Current was well extended into the GoM, but it was still south of the Macondo platform position (marked by red dot). The front of the anticyclonic Loop Current was surrounded by frontal cyclones and anticyclones. In the following weeks, the Loop Current evolved due to the growth of a cyclone on its eastern side that led to the detachment of a large anticyclonic Loop Current Eddy, named Eddy Franklin [20], around day 150. According to our computation, this Eddy is totally separated at the end of June. Eddy Franklin separation resulted in a southward position of the Loop Current, and together with local southeasterly winds blowing in the period of the BP accident, effectively eliminated connectivity between the Northern Gulf and the Florida Straits.

4.2 Modeling BP Oil Spill

Figure 5 shows the sequence of integral[2] oil concentration snapshots at the sea surface predicted for year days 125, 137, 155, and 170. The concentration patterns indicate the advection of droplets by adjacent cyclonic and anticyclonic eddies. Weak winds during May 16–19, and northward bulging of the Loop Current resulted in Macondo oil entrainment into the Loop current and its transport far to the southeast, as shown in Figure 5 (day 137). For comparison, we present, in Figure 6, the visible satellite image of the oil slick taken on 17 May 2010. As seen, a long ribbon of oil stretched from the main area of the spill far to the southeast. Apparently that it was the attenuation of southwesterly winds that allowed the Loop Current to drag the oil toward the Florida Strait.

In June (days 155 and 170), oil slick was entrained into the Loop Current outer edge by cyclonic and anticyclonic frontal eddies, while some amount of oil entering the Loop Current headed to the Florida Strait. Comparing with satellite imagery, our model simulation correctly showed that a lot of the surface oil was pushed ashore, contaminating Louisiana, Alabama and Florida panhandle region coasts.

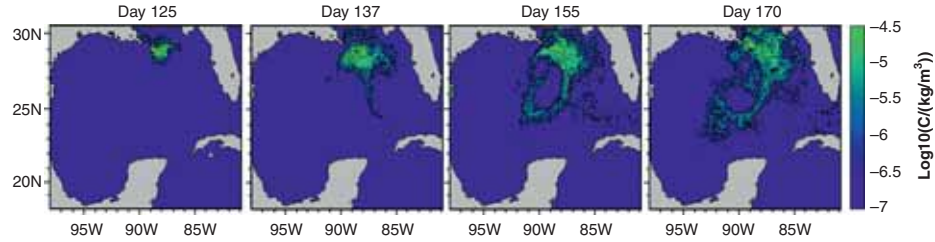

Figure 5 Sequence of the oil droplet concentration snapshots computed for year days as in Figure 4.

[2] Droplets within upper 0–300 m layer.

DOI: 10.7569/JSEE.2012.629504

Figure 6 Visible image of Deepwater Horizon oil spill slick 17 May 2010. (Credit: NASA image by Jeff Schmaltz, MODIS Rapid Response Team).

Our simulations also predict realistic locations of the oil landfall, mainly around the Mississippi Delta, then south of Louisiana and along the Mississippi and Alabama coastlines and then along the northeastern Florida coasline. This is in good agreement with observed oil impact along the northeastern Gulf coast. A similar result was obtained recently in [20].

In stark contrast to the simulations with synoptic wind forcing, testing simulations (not shown) without such synoptic wind forcing indicated that the oil slick had a tendency to move southward in result of advection by the neighboring cyclonic eddy (Figure 4, day 125). The southward advection of oil, intensified during the following weeks by the Loop Current, resulted in that the major amount of oil penetrated into the Atlantic Ocean through the Florida Strait while only a minor amount of oil reached the northeastern Gulf coasts.

Figure 7 illustrates a 3-D distribution of oil droplets released from the Macondo well during 60 days following the BP Deepwater Horizon blowout. Since currents throughout the major part of the water column, predicted by the DieGOM and confirmed by recent observations [3], are weak ($< 0.1 ms^{-1}$), the rapid rise of oil droplets will form a vertical plume (up to 1000) m above the Macondo wellhead. At the same time, an influence of subsea crosscurrents on ascending plume is clearly seen, even in case of large terminal velocities. The horizontal deviation of droplet positions from the vertical axis, as Figure 7 reveals, varies from 1 to 5 grid cells (14–70 km). In the upper 400 m layer, the oil plume structure is formed under the influence of cyclonic and anticyclonic eddies. At the sea surface, a major role

DOI: 10.7569/JSEE.2012.629504

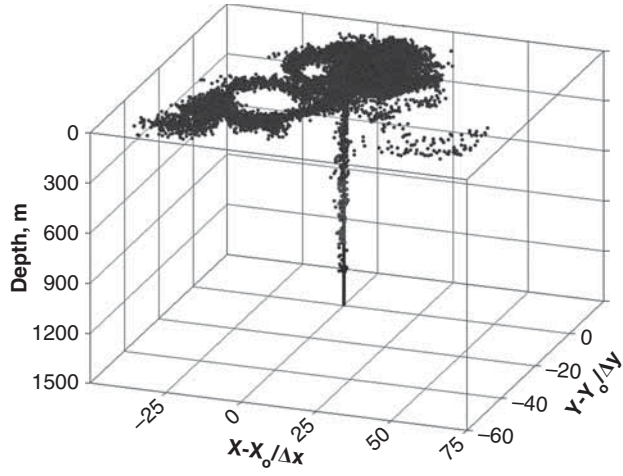

Figure 7 3-D distribution of oil droplets released from the Macondo oil well for 60 days after the accident. Horizontal scales are given in a number of cells away from the location of Macondo wellhead (X_O, Y_O). *X*, *Y* are the current position of a droplet occurred in a cell with resolution $\Delta x, \Delta y$.

in distribution of oil droplets is played by wind and wave drift, which push the oil slick ashore.

5 Conclusion

A well validated fourth-order-accurate z-level DieCAST ocean model, including its coupling to a full featured oil transport model, is used to simulate the GoM flow over a range of time scales from days to a century. We focused on hindcast of the transport and dispersal of oil from the BP Oil Spill in 2010. We simulated the GoM dynamics and a 3-D distribution of oil for the period of accident, as well as showing that synoptic winds played a crucial role in driving the surface oil slick toward the northeastern GoM coastlines. The NARR winds data show that dominant northwestward winds during the first 25 days (April 20–May 15) of the blowout prevented oil from reaching the Loop Current in the early stage of the spill. Soon after, the simulations indicate quick southward spreading of a surface oil ribbon (Figures 5, 6) entrained into the outer fringes of the Loop Current, due to decreased northwestward winds during May 16–20 (Figure 2). By the end of May and during June, the winds turn to northwestward again, pushing the surface oil along the northeastern GoM coastlines, as seen on days 155 and 170 (Figure 6). As was also found in [20], in our work, besides the prediction of the 3-D rising Macondo plume, after the blowout material reaches the surface, the high variability of wind and wave drift current significantly influences the predictability of oil slick transport due to limited weather forecasting predictability.

DOI: 10.7569/JSEE.2012.629504

5.1 Future Work That Needs to be Done

Herein, we have focused on the surface plume evolution on a short (few months) time scale, in the absence of oil material bonding to dispersants. Addressing the effects of dispersant bonding to blowout material requires detailed microphysics described by special algorithms that describe the alteration the physical properties of the combined bulk material that change its transport and fate [36], which are not included in this preliminary study. Using dispersants does not reduce the amount of oil entering the environment; instead, dispersants alter the oil droplet size distribution [38], buoyancy, and equilibrium depth of the bulk material consisting of dispersant bonded to blowout material. Lots of the oil material settles to deep equilibrium levels (where it is neutrally buoyant) based on Archimedes' Law combined with the fact that GoM water density increases monotonically with increasing depth. Much of it is found at an equilibrium depth of 1200 meters [7, 8, 12, 36].

Chemical dispersants significantly transform oil droplet size distribution so that the number of large and very large droplets (200–400 μm) decreases, while the number of small and very small droplets (2–12 μm) greatly increases. The dispersants result in material elements of dispersant material bonded to blowout material, generally increasing the bonded material bulk density, making it denser than surface water, so it does not accumulate at the surface. Instead, it migrates to a level where its bulk density matches the GoM water density according to Archimedes' Law. The associated microscale vertical churning leads to a much reduced upper level oil concentration. This reduces the amount of material that is wind blown ashore *in the short run*. However, it is still in the GoM, at subsurface levels, much of it below thermocline and Florida Strait sill depths (about 700 m). Buoyancy and rotation constraints trap such dense deep material in the GoM for decades to centuries, as the typical residence time of subthermocline water is 250 years [39, 40].

Bonded material having density greater than thermocline level GoM water floats around for decades to centuries in its sub-thermocline equilibrium depth. The positive chemical dispersal effect is thus that a large amount of oil does not reach the sea surface; however, after reaching its subsurface equilibrium level, it is dispersed laterally by deep currents, but not vertically, due to buoyancy and rotation constraints except during hurricane events, such as category 1 hurricane Isaac, which churned up deep blowout material in tarballs and blew them ashore [41]. Thus, dense bonded material suspended at depths below the surface mixed layer, especially below the thermocline, represents a 'ticking bomb' that will explode during future hurricanes passing over the GoM.

Hurricane eye wall winds drive the upper layer water outward as centrifugal and Coriolis acceleration dominate. This forces deeper water, under the eye wall, up to the surface to replace the upper layer water. That means it converges laterally at deeper levels, bringing with it dense deep water with suspended

DOI: 10.7569/JSEE.2012.629504

blowout material toward the eye wall and lifting it to the surface. It is a gigantic pumping and churning action [42]. The power of a hurricane is enough to lift great amounts of dense thermocline level to the surface in a short time. Even a category 1 typhoon churned thermocline level water up to the surface [43]. The amount of material increases with hurricane intensity and lateral extent from which suspended material converges to the region underlying the eye wall; and slower moving hurricanes also favor more tarballs being raised to the surface and blown ashore.

Thus, the long-term equilibrium depth distribution of the oil depends mainly on the material density of the bonded dispersant and blowout material elements. That, in turn, depends on the ratio of dispersant to oil blowout material. Modeling that requires special chemical and physical process information, which is not addressed in this preliminary study. The blowout material does not mix with water. Thus, if it is not blown ashore or does not escape through the Florida Strait during a storm event, it will sink back to an equilibrium depth after a hurricane event. Further, the chemical dispersants may delay or stop biodegradation of the suspended material. Statistically, one would expect most of the blowout material to end in the wetlands and other coastal regions, rather than escape through the Florida Strait, because the escape route through the Florida Strait is so narrow compared to the long GoM coastline. The problem touched above is very interesting for future work that will be directed to modeling the long term paths and dispersion of dense blowout material bonded to the dispersant, having buoyancy equilibrium at subthermocline depths.

Acknowledgements

Authors are thankful to P. Carmical for his kind invitation to submit a paper to the first issue of the Journal.

References

1. C.J. Cleveland, C.M. Hogan, and P. Saundry, Deepwater Horizon oil spill, in *Encyclopedia of Earth*, C.J. Cleveland, (Ed.), Environmental Information Coalition, National Council for Science and the Environment, Washington, DC (2010).
2. K. Korotenko, M. Bowman, and D. Dietrich, Oceanographers and modelers learning to track and predict Gulf oil spill plume. *J. Cosmology* **8**, 2023 (2010).
3. E.A. Norse and J. Amos, *Impacts, Perception, and Policy Implications of the Deepwater Horizon Oil and Gas Disaster*, pp. 11058, Environmental Law Institute, Washington, DC 40 ELR (2010).
4. M. McNutt, R. Camilli, G. Guthrie, P. Hsieh, V. Labson, B. Lehr, D. Maclay, A. Ratzel, and M. Sogge, Assessment of flow rate estimates for the Deepwater Horizon / Macondo Well Oil Spill. in Flow rate technical group report to the National Incident Command, Interagency Solutions Group, March 10, 2011, pp. 1–22, (2011)

DOI: 10.7569/JSEE.2012.629504

5. B. Lehr, S. Bristol, and A. Possolo, Oil budget calculator—deepwater horizon, federal interagency solutions group, oil budget calculator science and engineering team, pp. A2.1–A2.10 (2010). http://www.restorethegulf.gov/sites/default/files/documents/ pdf/OilBudgetCalc_Full_HQ-Print_111110.pdf (As of November 2012).
6. T.J. Crone1 and M. Tolstoy, Magnitude of the 2010 Gulf of Mexico oil leak. *Science* **330**, 634 (2010).
7. R. Camilli, C.M. Reddy, D.R. Yoerger, B.A.S. Van Mooy, M.V. Jakuba, J.C. Kinsey, C.P. McIntyre, S.P. Sylva, and J.V. Maloney, Tracking hydrocarbon plume transport and biodegradation at Deepwater Horizon. *Science* **330**, 201 (2010).
8. T.C. Hazen, E.A. Dubinsky, T.Z. DeSantis, G.L. Andersen, Y.M. Piceno, N. Singh, J.K. Jansson, A. Probst, S.E. Borglin, J.L. Fortney, W.T. Stringfellow, M. Bill, M.E. Conrad, L.M. Tom, K.L. Chavarria, T.R. Alusi, R. Lamendella, D.C. Joyner, C. Spier, J. Baelum, M. Auer, M.L. Zemla, R. Chakraborty, E.L. Sonnenthal, P. D'Haeseleer, H.-Y.N. Holman, S. Osman, Z. Lu, J.D. Van Nostrand, Y. Deng, J. Zhou, and O.U. Mason, Deep-sea oil plume enriches indigenous oil-degrading bacteria. *Science* **330**, 204 (2010).
9. P. Burgherr, In-depth analysis of accidental oil spills from tankers in the context of global spill trends from all sources. *J. Hazard. Mater* **140**, 245 (2007).
10. V. Klemas, Tracking oil slicks and predicting their trajectories using remote sensors and models: case studies of the sea princess and Deepwater Horizon oil spills. *J. Coast. Res* **26**(5), 789 (2010).
11. S.A. Socolofsky and E.E. Adams, Multi-phase plumes in uniform and stratified crossflow. *J. Hydraul. Res* **40**, 661 (2002).
12. S.A. Socolofsky, E.E. Adams, and C.R. Sherwood, Formation dynamics of subsurface hydrocarbon intrusions following the Deepwater Horizon blowout. *Geophys. Res. Lett* **38**, L09602 (2011).
13. S.M. Masutani and E.E. Adams, Experimental Study of Multi-Phase Plumes with Application to Deep Ocean Oil Spills, in *Final Report*, *U.S. Department of the Interior Minerals Management Service*, Washington, DC, Contract No. 1435-01-98-CT-30964 (2000). http://www.mms.gov/tarprojects/377.htm
14. L.K. Dasanayaka and P.D. Yapa, Role of plume dynamics phase in a deepwater oil and gas release model. *J. Hydro-Environm. Res* **2**, 243 (2009).
15. E.W. North, E.E. Adams, Z. Schlag, C.R. Sherwood, R. He, K.H. Hyun, and S.A. Socolofsky, Simulating oil droplet dispersal from the Deepwater Horizon spill with a Lagrangian approach. *Geophys. Monogr. Ser* **195**, 217 (2011).
16. A. Adcroft, R. Hallberg, J.P. Dunne, B.L. Samuels, J.A. Galt, C.H. Barker, and D. Payton, Simulations of underwater plumes of dissolved oil in the Gulf of Mexico. *Geophys. Res. Lett* **37**, L18605 (2010).
17. Y. Liu, R.H. Weisberg, C Hu, and L. Zheng, Tracking the Deepwater Horizon oil spill: A modeling perspective. *EOS* **92**(6), 45 (2011).
18. O.Yu. Lavrova and A.G. Kostianoy, Catastrophic oil spill in the Gulf of Mexico in April–May 2010. Izvestiya. *Atmos. Oceanic. Phys* **47**, 1114 (2011).
19. M.J Bowman, D.E. Dietrich, K.A. Korotenko, and M.H. Bowman, Modeling of circulation and dispersal of oil from the Deepwater Horizon blowout in the Gulf of Mexico. In Proc. Gordon Res. Conf. July 4–7, Kingston, RI, USA, (2011).

DOI: 10.7569/JSEE.2012.629504

20. M. Le Hénaff, V.H. Kourafalou, C.B. Paris, J. Helgers, Z.M. Aman, P.J. Hogan, and A. Srinivasan, Surface evolution of the Deepwater Horizon oil spill patch: Combined effects of circulation and wind-induced drift. *Environ. Sci. Technol* **46**, 7267 (2012).
21. S.L. Ross Environmental Research Ltd., Fate and Behavior of Deepwater Subsea Oil Well Blowouts in the Gulf of Mexico, in *Report 287AA, U.S. Department of the Interior Minerals Management Service,* Washington, DC, pp. 1–25 (1997).
22. O. Johansen, DeepBlow—a Lagrangian plume model for deep water blowouts. *Spill. Sci. Technol Bull* **6**, 103 (2000).
23. M.L. Spauding, P.R. Bishnoi, E. Anderson, T. Isaji, An integrated model for prediction of oil transport from a deep water blowout. in 23rd AMOP Technical Seminar 2000, June 14– 16, 2000, Ottawa, Canada, 2, 611 (2000)
24. L. Zheng and P.D. Yapa, Buoyant velocity of spherical and nonspherical bubbles/droplets. *J. Hydraulic. Engineer. ASCE* **124**, 852 (2000).
25. L. Zheng, P.D. Yapa, and F. Chen, A model for simulating deepwater oil and gas blowouts -Part I: Theory and model formulation. *J. Hydraulic. Res* **41**, 339 (2003).
26. F. Chen and P.D. Yapa, Modeling gas separation from a bent deepwater oil and gas jet/plume. *J. Mar. Syst* **45**, 189 (2004).
27. R.H. Perry and D.W. Green, *Percy's Chemical Engineers' Handbook*, 6th Edition, McGraw Hill Book Co., New York, NY (1984).
28. R.B. Wheeler, *The Fate of Petroleum in the Marine Environment*, Special Report, Exxon Production Research Co., Houston, USA pp. 1–124 (1978).
29. K.A. Korotenko, R.M. Mamedov, and C.N.K. Mooers, Prediction of the dispersal of oil transport in the Caspian Sea resulting from a continuous release. *Spill. Sci. Technol. Bull* **6**, 323 (2000).
30. K.A. Korotenko, R.M. Mamedov, A.E. Kontar, and L.A. Korotenko, Particle tracking method in the approach for prediction of oil slick transport in the sea: modeling oil pollution resulting from river input. *J. Mar. Syst* **48**, 159 (2004).
31. K. Korotenko, M. Bowman, and D. Dietrich. High-resolution model for predicting the transport and dispersal of oil plumes resulting from accidental discharges in the Black Sea. Terr. Atmos. Ocean. Sci 21, 123 (2010).
32. A.J. Elliott, Shear diffusion and the spread of oil in the surface layers of the North Sea. *Dt. Hydrogr. Z* **39**, 113 (1986).
33. D. Mackay and C. McAuliffe, Fate of hydrocarbons discharged at sea. *Oil Chem. Pollution* **5**, 1 (1988).
34. D. Daling, The weathering properties of the Macondo crude at sea in the GoM and the effectiveness of surface and sub-surface dispersant application, Personal communication, http://www.cedre.fr/en/publication/jourinfo11/2-SINTEF_gb.pdf (2011).
35. M. Fingas and B.F.J. Mullin, Water-in-oil emulsions results of formation studies and applicability to oil spill modeling. *Spill. Sci. Technol. Bull* **5**, 81 (1999).
36. J.L. Ramseur, Deepwater Horizon oil spill: The fate of the oil. in Rep. R41531, *CRS* **7–5700**, 1–20 (2010).
37. D. Mackay and R. Matsugu, 1973, Evaporation rate of liquid hydrocarbon spills on land and water. *Can. J. Chem. Eng* **51**, 43 (2010).
38. B. Lehr, S, Bristol, and A. Possolo, Oil budget calculator—deepwater horizon, federal interagency solutions group, oil budget calculator science and engineering

DOI: 10.7569/JSEE.2012.629504

team, (2010). http://www.restorethegulf.gov/sites/default/files/documents/pdf/OilBudgetCalc_Full_HQ-Print_111110.pdf (as of November 1, 2012).
39. D.M. Fratantoni, R.J. Zantopp, W.E. Johns, and J.L. Miller, Updated bathymetry of the Anegada-Jungfern Passage complex and implications for Atlantic inflow to the abyssal Caribbean Sea. *J. Marine Res* **55**, 847 (1997).
40. D. Rivas, A. Badan, J. Ochoa, The ventilation of the deep Gulf of Mexico. *J. Phys. Oceanogr* **35**, 1763 (2005).
41. news.discovery.com, http://news.discovery.com/earth/isaac-churned-up-bp-tar-balls-120913.html (2012).
42. Q. Schiermeier, Oceanography: Churn, Churn, Churn. *Nature*, **447**, 522 (2007).
43. Y.-H. Tseng, S. Jan, D. Dietrich, I-I. Lin, Y.-T. Chang, and T.Y. Tang, Modeled oceanic response and sea surface cooling to typhoon Kai-Tak. *Terr. Atmos. Sci* **21**, 85 (2010).

DOI: 10.7569/JSEE.2012.629504